

A THEORY OF BUNCH LENGTHENING IN ELECTRON STORAGE RINGS WITH LOCALIZED WAKE FORCE SOURCES

KOHI HIRATA

*National Laboratory for High Energy Physics, Oho-machi, Tsukuba-gun,
Ibaraki-ken, 305, Japan*

(Received April 24, 1986; in final form October 21, 1986)

The longitudinal motion of electrons in a storage ring cannot be described correctly with the usual Fokker–Planck equation when a wake force is fully local, unless some complicated regularization is performed. Instead, a mapping formulation is proposed which is based on a complete description of the behavior of the distribution function. With some approximation, the method leads to a set of mapping equations for a few parameters. As an example, a simple soluble model is constructed which turns out to show good qualitative agreement with multiparticle tracking, but qualitative disagreement with conventional theory.

1. INTRODUCTION

The bunch lengthening or the longitudinal motion of particles in a bunch is more or less perturbed by the wake force.¹ The sources of the wake force, cavities, bellows, etc., are distributed throughout the ring. Each of the sources is a highly localized object. It is, thus, natural to regard the wake force field felt by individual particles as time dependent (time being a position in a ring). In analytical treatments, however, the wake force is almost always averaged over one turn.

On the other hand, multiparticle tracking (MPT, a powerful tool for studying the wake effect) almost always treats the wake force as working at one point in a ring (or in one superperiod). This is partly because the calculation time is limited and partly because the symplecticity is easily assured. In this respect, conventional analytical theory and multiparticle tracking are possibly different from one another. In fact, there is a qualitative difference between predictions given by the two methods for at least one simple example,² which will be recapitulated later in this paper.

It seems convenient for us here to summarize the characteristic points of the conventional theory: When the current I is less than a threshold current I_{th} , the bunch is governed by a static solution of the Fokker–Planck (FP) equation.³ This solution will be called the potential-well distortion (PWD) equation, since it, itself, is a complicated integral equation. When $I > I_{th}$, this basic distribution becomes unstable; a mode coupling⁴ occurs and the corresponding collective motion blows up.

When the wake force field is to be treated as time dependent, in particular, as

in the case of MPT, we cannot use the static solution of the PWD equation as the basic distribution. It is, therefore, desirable to construct an analytical theory which incorporates the time dependence. Since a delta functional time dependence is most tractable, we shall confine ourselves to such a case. However, it seems quite difficult to construct a general theory. In this paper, we instead present a simple soluble model as a starting point.

In the next section, it will be shown that we cannot extend the usual FP equation by simply employing the time-dependent effective Hamiltonian. Section 3 is then devoted to the presentation of an alternative method and its application to a simple example. Also, a relation of the new method to the PWD equation is given. An additional discussion is given for the PWD equation in Section 4. In the final section, we discuss our results in connection with MPT and conventional theory. We also give a conjecture for general cases and present a problem concerning actual storage rings. Detailed discussions are relegated to appendices.

2. FUNDAMENTAL CONCEPTS

In this section, after establishing the notation, we discuss the compatibility of the localized wake force and the FP equation. For the sake of simplicity, we assume that the classical part (i.e., the part without radiation effects) of the dynamics for an individual particle can be described by a Hamiltonian

$$H = H_0 + H_1 \delta(\theta), \quad (1)$$

$$H_0 = \frac{v_s}{2} (x_1^2 + x_2^2), \quad (2)$$

$$H_1 = \int_0^{x_1} f(x_1) dx, \quad (3)$$

$$f(x_1) = \frac{1}{E_0} \int_0^\infty \rho(x_1 - u) W_L(u) du, \quad (4)$$

where $\delta(\theta)$ is a periodic delta function with period 2π , θ is the “time” (arc length/mean radius),

$$x_1 = \frac{\omega_s}{\alpha} \tau,$$

$$x_2 = \varepsilon = \frac{E - E_0}{E_0},$$

and other symbols are as defined in Table I. Here the effect of acceleration is treated as averaged over one turn. Since this effect belongs to a linear dynamics, it produces no unphysical results, as long as the force is treated as a harmonic oscillator-like force.

Let us summarize the usual treatment, which uses the time-averaged Hamiltonian

$$\bar{H} = H_0 + \frac{1}{2\pi} H_1. \quad (5)$$

TABLE I

Symbols and their definitions. In numerical evaluations shown later, we used the listed model values.

Symbol	Definition	Model value
α	Momentum compaction factor	0.72015×10^{-3}
ω_s	Synchrotron frequency	
ν_s	Synchrotron tune	0.091327
E_0	Beam energy, nominal (GeV)	25
τ	Delay of a particle (s)	
ε	Energy deviation of a particle	
E	Energy of a particle	
T_e	Damping time in turns	178.5
σ_0	Nominal energy spread	1.36×10^{-3}
ρ	Charge density	
W_L	Longitudinal wake function	
ψ	Normalized distribution function	
Q_{tot}	Total charge of a bunch	
N_s	Superperiodicity	
N_p	Number of super-particles in a bunch for multiparticle tracking	4000

The FP equation is

$$\frac{\partial \psi}{\partial \theta} \equiv \dot{\psi} = [\bar{H}, \psi] + \frac{\partial}{\partial x_2} (\beta x_2 \psi) + D \frac{\partial^2 \psi}{\partial x_2^2}, \quad (6)$$

where $[,]$ is the Poisson bracket defined by

$$[f, g] = \frac{\partial f}{\partial x_1} \frac{\partial g}{\partial x_2} - \frac{\partial f}{\partial x_2} \frac{\partial g}{\partial x_1}, \quad (7)$$

$\beta = \pi/T_e$, $D = \beta\sigma_0^2$, and ψ is the normalized distribution function in one-particle phase space. Since \bar{H} is time independent, the FP equation has a static solution given by

$$\psi(x_1, x_2) = \psi_0 \exp\left(-\frac{\bar{H}}{\nu_s \sigma_0^2}\right), \quad (8)$$

which is the PWD equation (ψ_0 is the normalization constant).

Now, returning to H , Eq. (1), the dynamics is equivalent to the successive operation of the following three mappings.

$$\text{Oscillation} \quad \begin{pmatrix} x'_1 \\ x'_2 \end{pmatrix} = \begin{pmatrix} \cos \Delta\phi & \sin \Delta\phi \\ -\sin \Delta\phi & \cos \Delta\phi \end{pmatrix} \begin{pmatrix} x_1 \\ x_2 \end{pmatrix}, \quad (9)$$

where $\Delta\phi = 2\pi\nu_s$.

$$\text{Radiation} \quad \begin{aligned} x'_1 &= x_1, \\ x'_2 &= \xi x_2 + (1 - \xi^2)^{1/2} \sigma_0 \hat{P}, \end{aligned} \quad (10)$$

where

$$\xi = \exp(-2/T_e)$$

and \hat{P} is a Gaussian random noise with $\langle \hat{P} \rangle = 0$, $\langle \hat{P}^2 \rangle = 1$.

Wake

$$\begin{aligned} x'_1 &= x_1, \\ x'_2 &= x_2 - f(x_1). \end{aligned} \quad (11)$$

In the above, we treated the effect of radiation as localized at one point of the ring. Since, essentially, this effect also belongs to a linear dynamics, it produces no unphysical results. On the other hand, the localization of the source of the wake force may possibly produce a large difference from the continuously distributed source, since the force is highly nonlinear. We further assume that $W_L(t)$ decays so rapidly that the multiturn effect is negligible. This picture of considering a succession of operations is the same as that employed in MPT but different from the usual treatment based on the time-averaged Hamiltonian.

Notice here that this set of mappings is almost equivalent to the Langevin (or stochastic) equation

$$\frac{dx_1}{d\theta} = [x_1, H], \quad (12)$$

$$\frac{dx_2}{d\theta} = [x_2, H] - \beta x_2 + (2D)^{1/2} \hat{r}(\theta), \quad (13)$$

where \hat{r} is a noise with $\langle \hat{r} \rangle = 0$, $\langle \hat{r}(\theta) \hat{r}(\theta') \rangle = \delta(\theta - \theta')$. Here, however, δ is the usual (not periodic) delta function.

It is evident that we cannot track the behavior of an individual particle. We had better confine our studies to some statistical quantities such as

$$\begin{aligned} X_i &= \langle x_i \rangle, \\ \sigma_{ij} &= \langle (x_i - X_i)(x_j - X_j) \rangle, \\ \sigma_{ijk} &= \langle (x_i - X_i)(x_j - X_j)(x_k - X_k) \rangle, \end{aligned} \quad (14)$$

(i, j, k being 1 or 2) and so on. According to Eqs. (9)–(11), the variation of these quantities are given as follows:

Oscillation

$$\begin{aligned} X'_i &= \sum_j U_{ij} X_j, \\ \sigma'_{ij} &= \sum_{l, m} U_{il} \sigma_{lm} U_{mj}^{-1}, \end{aligned} \quad (15)$$

$$U = \begin{pmatrix} \cos \Delta\phi & \sin \Delta\phi \\ -\sin \Delta\phi & \cos \Delta\phi \end{pmatrix}.$$

Radiation

$$\begin{aligned} X'_1 &= X_1, \\ X'_2 &= \xi X_2, \\ \sigma'_{11} &= \sigma_{11}, \\ \sigma'_{12} &= \xi \sigma_{12}, \\ \sigma'_{22} &= \xi^2 \sigma_{22} + (1 - \xi^2) \sigma_0^2. \end{aligned} \quad (16)$$

$$\begin{aligned}
\text{Wake} \quad X'_1 &= X_1, \\
X'_2 &= X_2 - \langle f \rangle, \\
\sigma'_{11} &= \sigma_{11}, \\
\sigma'_{12} &= \sigma_{12} - \langle (x_1 - X_1)f \rangle, \\
\sigma'_{22} &= \sigma_{22} - 2\langle (x_2 - X_2)f \rangle + \langle f^2 \rangle - \langle f \rangle^2,
\end{aligned} \tag{17}$$

where $\langle \rangle$ indicates the average over all particles,

$$\langle g \rangle = \int dx_1 dx_2 g(x_1, x_2) \psi(x_1, x_2) \tag{18}$$

for any function $g(x_1, x_2)$. Variations of other higher-order moments can also be given easily. Notice that the averages in Eq. (17) should be evaluated with ψ evaluated just before the *Wake* mapping.

For later convenience, it seems useful here to pay attention to how σ'_{22} in Eq. (17) is derived:

$$\langle x_2 \rangle_- \rightarrow \langle x_2 \rangle_+ = \langle x_2 \rangle_- - \langle f \rangle_-, \tag{19}$$

$$\begin{aligned}
\langle x_2^2 \rangle_- \rightarrow \langle x_2^2 \rangle_+ &= \langle [x_2 - f(x_1)]^2 \rangle_- \\
&= \langle x_2^2 \rangle_- - 2\langle x_2 f(x_1) \rangle_- + \langle f^2 \rangle_-,
\end{aligned} \tag{20}$$

where $\langle \rangle_+$ and $\langle \rangle_-$ are the averages after and before $\theta = 0$, respectively.

Now let us try to rederive the results using the FP equation with the classical Hamiltonian H simply by replacing \bar{H} in Eq. (6) with H . In the vicinity of the source of the wake force, we need only consider the H_1 term, since other factors in the FP equation are continuous in θ , and their effect on the change of ψ from $\theta = 0^-$ to 0^+ is infinitely small:

$$\dot{\psi} = [H_1, \psi] \delta(\theta) = \frac{\partial \psi}{\partial x_2} f(x_1) \delta(\theta); \quad (\theta \cong 0). \tag{21}$$

It can be easily seen that Eq. (21) is self-contradicting. [We will not use Eq. (21) in subsequent sections. Those who are not interested in the danger of Eq. (21) can skip the following and proceed directly to Section 3.]. We expect ψ to change discontinuously at $\theta = 0$; thus, $\psi = \psi(0^+) \Theta(\theta) + \psi(0^-) \Theta(-\theta)$ near $\theta \cong 0$, where Θ is the unit step function. The right-hand side of Eq. (21) thus contains a product of two distributions (generalized functions). It is well-known that we must be careful with such a product. In fact, it is easy to show that a formal application of Eq. (21) leads to ill defined (and incorrect) expressions.

It is true that this equation gives an accurate formula for $X_2 = \langle x_2 \rangle$:

$$\begin{aligned}
\frac{dX_2}{d\theta} &= \int x_2 \dot{\psi} dx_1 dx_2 \\
&= \int x_2 \frac{\partial \psi}{\partial x_2} f(x_1) \delta(\theta) dx_1 dx_2 \\
&= - \int \psi f(x_1) \delta(\theta) dx_1 dx_2 \\
&= - \langle f \rangle \delta(\theta),
\end{aligned} \tag{22}$$

and this gives $X_2' = X_2 - \langle f \rangle$ after integration of θ , since $\langle f \rangle$ is continuous at $\theta = 0$. For $\langle x_2^2 \rangle$, however, Eq. (21) leads to an incorrect and ill-defined expression:

$$\begin{aligned} \frac{d}{d\theta} \langle x_2^2 \rangle &= \int x_2^2 \dot{\psi} dx_1 dx_2 \\ &= -2 \langle x_2 f \rangle \delta(\theta). \end{aligned} \quad (23)$$

First, the term $\langle f^2 \rangle$ is absent. Furthermore, the right-hand side contains a product of two distributions, since $\langle x_2 f \rangle$ has a discontinuity at $\theta = 0$.

It is clear that this difficulty comes from the formal extension of the ‘‘thin-lens approximation’’ for single-particle dynamics to the equation for ψ . The Hamiltonian H , Eq. (1), is suitable for the Langevin (or Hamilton) equation but not for the FP (or Vlasov) equation.

Let us regularize Eq. (21) by starting at a more fundamental level. Near $\theta = 0$, we have

$$\begin{aligned} \Delta x_1 &= 0, \\ \Delta x_2 &= -f(x_1) \Theta(\theta), \end{aligned} \quad (24)$$

according to Eq. (11). We can also derive Eq. (24) from Eqs. (12) and (13). From an obvious formula, namely the original expression for $d\psi/d\theta = 0$,

$$\psi(x_1, x_2, 0^+) = \psi(x_1 - \Delta x_1, x_2 - \Delta x_2, 0^-), \quad (25)$$

and Eq. (24), we can obtain

$$\begin{aligned} \psi(0^+) - \psi(0^-) &= \psi[x_1, x_2 + f(x_1), 0^-] - \psi(x_1, x_2, 0^-) \\ &= \left[\frac{\partial \psi}{\partial x_2} f(x_1) + \frac{1}{2} \frac{\partial^2 \psi}{\partial x_2^2} f^2(x_1) + \cdots \right]_{0^-}. \end{aligned} \quad (26)$$

That is, in our case, $(\Delta x_2)''$ is not negligible in comparison with $\Delta\theta$. Equation (26) suggests that a correct differential equation is not Eq. (21), but rather

$$\frac{\partial \psi}{\partial \theta} = \left\{ \lim_{\theta \rightarrow 0^-} \left[\frac{\partial \psi}{\partial x_2} f(x_1) + \frac{1}{2} \frac{\partial^2 \psi}{\partial x_2^2} f^2(x_1) + \cdots \right] \right\} \delta(\theta). \quad (27)$$

It is easy to see that Eq. (27), when applied to Eq. (23), gives Eq. (20). It is clear now that the usual FP equation, Eq. (6) with \bar{H} replaced by H , gives a correct kick only for a dipole mode X_i [Ruggiero⁵ gives a regularization of Eq. (23), which can reproduce Eq. (20) as well as Eq. (19). However, it does not apply to higher-order moments. See Appendix A]. In general, however, the dipole kick $\langle f \rangle$ depends on all modes of ψ . The usual FP equation thus leads to incorrect results, even for the dipole mode, except for very exceptional cases. We show an alternative regularization of Eq. (21) in Appendix B. [Other papers^{6,7} have used the Vlasov equation with an H-type time-dependent Hamiltonian, Eq. (1), in other contexts. The validity of such uses should be examined carefully.]

Thus, we cannot use the usual FP equation in the case of the localized wake force. If we insist on using a differential-type equation, we must employ the

following generalized FP equation:

$$\frac{\partial \psi}{\partial \theta} = [H_0, \psi] + \text{rhs. of Eq. (27)}$$

$$+ \text{additional part of Eq. (6)}. \quad (28)$$

Notice here also that Eq. (27) justifies the assertion given below Eq. (18).

Since Eq. (28) is very untractable, we had better restart from the mapping equations given by Eqs. (15)–(17). One of the possible methods and a simple soluble example are given in the next section.

3. A SOLUBLE MODEL

If we knew all of the moments such as X_i , σ_{ij} , σ_{ijk} , at the n th turn, we could reconstruct $\psi^{(n)}(x_1, x_2)$. Then, the next wake kicks, such as $\langle f \rangle$, $\langle f^2 \rangle$, $\langle f^3 \rangle$, . . . , could be obtained so that we find $\psi^{(n+1)}(x_1, x_2)$. Actually, however, we are forced to work with a few lower-order moments. In such a case, the reconstruction is not unique. There may be several methods to do this systematically. In this paper, we employ a simple, but not trivial, assumption that ψ can always be expressed as

$$\psi(x_1, x_2) = \frac{1}{2\pi\sqrt{\det \sigma}} \exp \left[-\frac{1}{2} \sum_{i,j} \sigma_{ij}^{-1} (x_i - X_i)(x_j - X_j) \right], \quad (29)$$

that is, we always replace a distorted ψ with the standardized ψ shown in Eq. (29). (See the discussion given in Section 5.3.)

It is desirable to work with a general wake function. This, however, seems quite difficult. In order to construct an analytically soluble model, we employ a constant wake, given by

$$W(u) = \begin{cases} W_0 H(V/C) & (0 < u < u_{\max}), \\ 0 & (\text{otherwise}), \end{cases} \quad (30)$$

where u_{\max} is much larger than the bunch length and indicates only that the multiturn effect is negligible.

Now our model is settled. Let us follow the variations of the parameters X_i , σ_{ij} for the operations given by Eqs. (15)–(17). The mean values appearing in Eq. (17) can be obtained analytically as follows:

$$\begin{aligned} \langle f \rangle &= f_0/2, \\ \langle f^2 \rangle &= f_0^2/3, \\ \langle (x_1 - X_1)f \rangle &= f_0 \sqrt{\sigma_{11}} / (2\sqrt{\pi}), \\ \langle (x_2 - X_2)f \rangle &= f_0 \sigma_{12} / (2\sqrt{\pi} \sigma_{11}). \end{aligned} \quad (31)$$

Here,

$$f_0 = \frac{W_0}{E_0} Q_{\text{tot}} \quad (32)$$

is a dimensionless parameter indicating the strength of the wake force.

Equation (31) leads to the remarkable fact that the mapping, Eqs. (15)–(17), becomes reducible: Mappings for X_i and for σ_{ij} become independent of one another. This is a special consequence of using a constant wake function and a Gaussian distribution function.

Let us first study the mapping for X_i . The mapping is linear and trivial:

Oscillation

$$X'_i = \sum_j U_{ij} X_j.$$

Radiation

$$X'_1 = X_1,$$

$$X'_2 = \xi X_2.$$

(33)

Wake

$$X'_1 = X_1,$$

$$X'_2 = X_2 - f_0/2.$$

On a Poincaré surface of section constructed just after *Oscillation* (just before *Radiation*), this system has a period-1 fixed point X_1^∞ :

$$\begin{aligned} X_1^\infty &= -\frac{f_0}{2 \tan(\Delta\phi/2)} \frac{1}{1 + \xi}, \\ X_2^\infty &= \frac{f_0}{2} \frac{1}{1 + \xi}. \end{aligned} \quad (34)$$

It is also easy to show that this fixed point is always stable (any X_i eventually goes down to X_i^∞). Thus, in our model, the dipole mode is always stable.

The mapping for σ_{ij} is not trivial:

Oscillation

$$\sigma' = U\sigma U^{-1}.$$

Radiation

$$\sigma' = \begin{pmatrix} \sigma_{11} & \xi\sigma_{12} \\ \xi\sigma_{12} & \xi^2\sigma_{22} + (1 - \xi^2)\sigma_0^2 \end{pmatrix}. \quad (35)$$

Wake

$$\sigma'_{11} = \sigma_{11},$$

$$\sigma'_{12} = \sigma_{12} - f_0\sqrt{\sigma_{11}}/(2\sqrt{\pi}),$$

$$\sigma'_{22} = \sigma_{22} - f_0\sigma_{12}/(\pi\sigma_{11})^{1/2} + f_0^2/12.$$

Let us first seek a period-1 fixed point σ_{ij}^∞ on the Poincaré surface of section constructed at the same position as before. After some algebra (see Appendix C), we obtain

$$\begin{aligned} (\sigma_{11}^\infty)^{1/2} &= -af_0 + [\sigma_0^2 + (a^2 + b)f_0^2]^{1/2}, \\ a &= \frac{\cot \Delta\phi}{2\pi^{1/2}(1 + \xi)}, \\ b &= \frac{\pi(1 - \xi) + (2\pi - 6)\xi}{12\pi(1 + \xi)(1 - \xi^2)}, \\ \sigma_{12}^\infty &= \frac{f_0}{2\pi^{1/2}(1 + \xi)} (\sigma_{11}^\infty)^{1/2}, \\ \sigma_{22}^\infty &= \sigma_0^2 + \frac{f_0^2}{12(1 - \xi^2)^2\pi} [(1 - \xi^2)\pi - 6\xi(1 - \xi)]. \end{aligned} \quad (36)$$

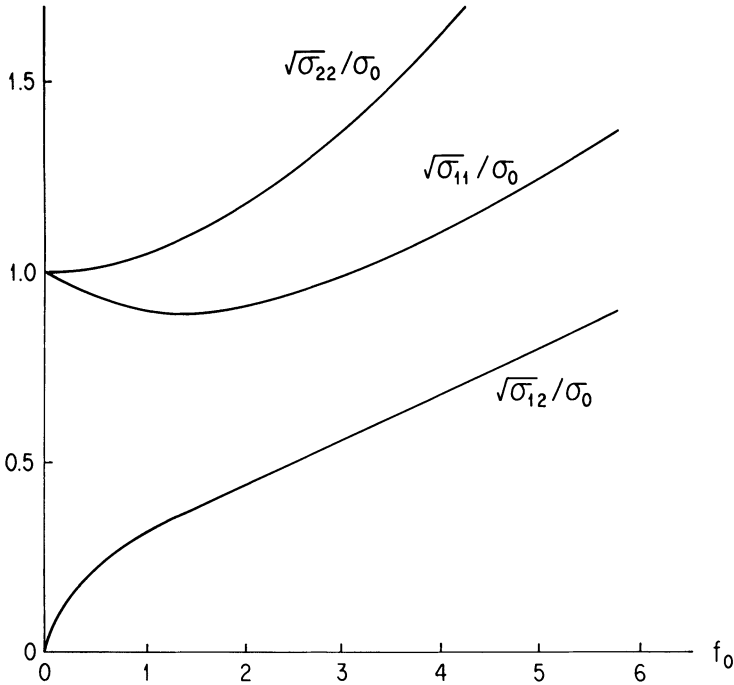


FIGURE 1 Period-one fixed points σ_{ij}^∞ of the mappings given by Eq. (35) as functions of the strength of the wake force. The parameters used are listed in Table I. The abscissa is labeled in units of 10^{-3} .

We show in Fig. 1 these points as functions of f_0 , using the numerical values listed in Table I.

It can be easily seen from Eq. (36) and Fig. 1 that (i) since $b > 0$, $(\sigma_{11}^\infty)^{1/2}$ is always positive and has a minimum at some value of f_0 ; (ii) σ_{22}^∞ grows quadratically as f_0 increases; and (iii) σ_{12}^∞ increases monotonically. It should be pointed out here that the mapping method for our simple model, given above, predicts qualitatively different behavior from that given by the PWD equation, Eq. (8), where the energy spread, $(\sigma_{22})^{1/2}$, must be constant and σ_{12} must be zero.

Lastly, in order to examine the stability of σ_{ij}^∞ analytically, one must solve a cubic eigenvalue equation. Here, we satisfy ourselves by knowing that numerical tracking of the mapping confirms that σ_{ij}^∞ is also stable, at least when f_0 is in the region shown in Fig. 1.

In the rest of this section, we shall further clarify the relation between our mapping method and the PWD equation. Let us introduce a superperiodicity N_s in our model. This is easily done by making the following substitutions in the mapping equations:

$$\begin{aligned} \Delta\phi &\rightarrow \Delta\phi/N_s, \\ \xi &\rightarrow \xi^{1/N_s}, \\ f_0 &\rightarrow f_0/N_s. \end{aligned} \quad (37)$$

The period-1 fixed points X_i^∞ , σ_{ij}^∞ remain fixed points.

On the other hand, it is almost certain that when N_s becomes large the effects of a discrete wake kick, given by Eq. (11), become smoother, so that the effect can be treated as a continuously applied force. In this limit, the usual FP equation, Eq. (6), works well. That is we can replace the time-dependent (i.e., θ -dependent) wake force by a ring-averaged θ -independent force. More exactly, in Eq. (27), $f(x_1)$ is replaced by $f(x_1)/N_s$, and if

$$f(x_1)/N_s \ll 1,$$

the higher-derivative terms in the generalized Vlasov equation become negligible.

In this case, the dynamics of X_i is described by distribution-averaged expression obtained from Eqs. (12) and (13), with H replaced by \bar{H} and with Eq. (37) taken into account, giving a set of differential equations instead of mapping difference equations:

$$\begin{aligned} \frac{dX_1}{d\theta} &= v_s X_2, \\ \frac{dX_2}{d\theta} &= -v_s X_1 - \frac{f_0}{4\pi} \end{aligned} \quad (38)$$

(as long as the Gaussian approximation is possible), which give a fixed point

$$(X_1, X_2) = \left(-\frac{f_0}{4\pi v_s}, 0 \right). \quad (39)$$

Naturally, from Eqs. (34) and (37), one can easily show that

$$\lim_{N_s \rightarrow \infty} (X_1^\infty, X_2^\infty)$$

is just the same as that given in Eq. (39).

The equilibrium distribution function (stable or unstable) is given by the PWD equation, Eq. (8). A bunch length σ_{11} , determined by the PWD equation, can be obtained numerically (see Section 4) and is compared to σ_{11}^∞ in Fig. 2 for various N_s . As $N_s \rightarrow \infty$, σ_{11}^∞ converges to the solution of PWD equation. In fact,

$$\lim_{N_s \rightarrow \infty} (\sigma_{11}^\infty)^{1/2} = -A + (\sigma_0^2 + A^2)^{1/2}, \quad (40)$$

$$A = \frac{f_0}{4\sqrt{\pi} \Delta\phi}, \quad (41)$$

fits the numerical solutions of the PWD equation surprisingly well. In Fig. 3, the convergence is shown for two fixed currents (wake force strengths). It is natural that the convergence is fast for low current.

As for σ_{12}^∞ and σ_{22}^∞ , it is easy to see that

$$\lim_{N_s \rightarrow \infty} \sigma_{12}^\infty = 0,$$

$$\lim_{N_s \rightarrow \infty} \sigma_{22}^\infty = \sigma_0^2,$$

the results being consistent with the PWD equation. Also, the fixed point X_1

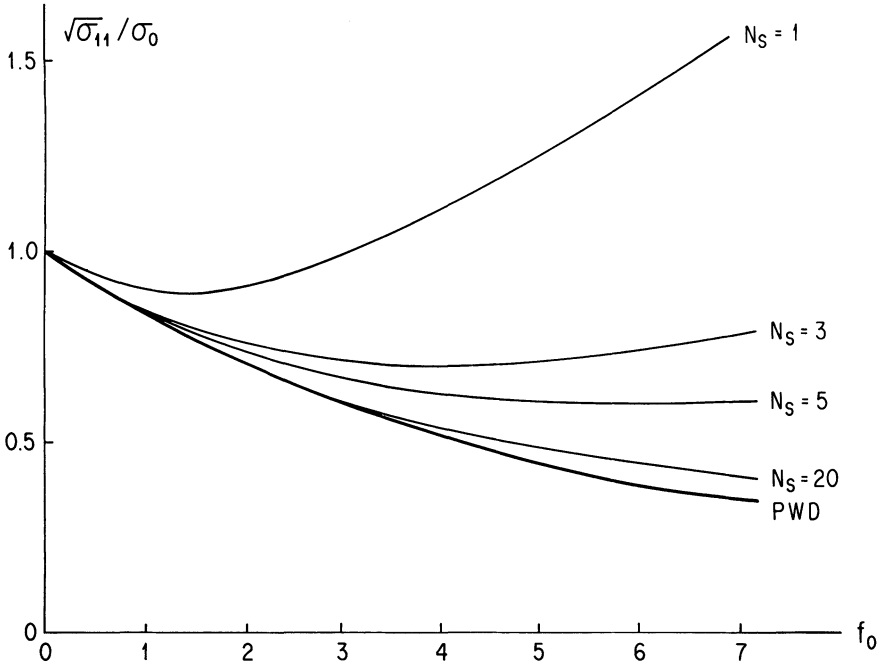


FIGURE 2 Fixed points σ_{11}^{∞} of the mapping for various N_s . As N_s increases the mapping curves approach the solution of the PWD equation. The solution for the PWD was obtained numerically. The abscissa is labeled in units of 10^{-3} .

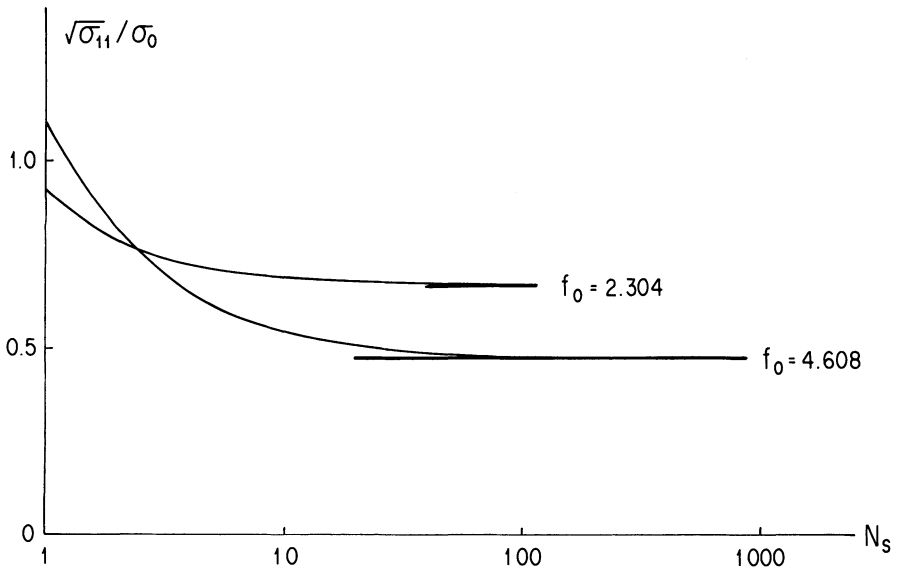


FIGURE 3 Fixed points σ_{11}^{∞} as a function of N_s with f_0 fixed. The value for f_0 are in units of 10^{-3} .

given by Eq. (39) is, of course, quite consistent with the numerical solution of the PWD equation.

The discussions above are enough to convince us that (i) where the wake source is highly localized (small N_s), the bunch length (and ψ) behave in a very different manner from that predicted by the usual FP equation using a ring-averaged wake force; and (ii) where the wake source is not so localized (large N_s) and the wake force is not so strong (low current), ψ can be treated in the conventional way. (See also the discussion in Section 5.2.)

4. THE POTENTIAL-WELL DISTORTION EQUATION

In this section, we discuss further the solution of the PWD equation. Although it is not the main aim of the present paper, it is interesting to see why Eq. (40) fits the numerical results of the PWD equation so well that there is no need to compare the two in a graph.

Let us begin by noticing the fact that the PWD equation, Eq. (8), is similar to the Boltzmann distribution (BD) if we regard $v_s\sigma_0^2$ as an effective temperature T :

$$T = v_s\sigma_0^2. \quad (42)$$

Given the distribution function ψ , we can define its entropy S (negative information) as

$$S = -\langle \ln \psi \rangle = -\int dx_1 dx_2 \psi \ln \psi. \quad (43)$$

Also the energy E of ψ is naturally given by

$$E = \langle \tilde{H} \rangle. \quad (44)$$

We can now introduce the free energy F by

$$F = E - TS. \quad (45)$$

When the Hamiltonian \tilde{H} is not the effective one but the usual one describing external force, it is easy to show that the BD is equivalent to an extremal condition of F . In our case, however, the PWD equation does not imply that F is a minimum, since \tilde{H} itself is a functional of ψ : $\tilde{H} = \tilde{H}[\psi]$. Let us temporarily write

$$\psi' = \psi_0 \exp(-\tilde{H}[\psi]/T). \quad (46)$$

Given ψ , ψ' is the most probable distribution (it minimizes F) under $\tilde{H}[\psi]$. In this respect, the PWD equation is a claim that

$$\psi' = \psi. \quad (47)$$

In numerically solving the PWD equation, we start with an approximate solution of Eq. (47), which is already given for a somewhat smaller f_0 , and apply Eq. (46) iteratively until Eq. (47) is achieved. The convergence is fast since we always give the most probable distribution for a given ψ , as long as there is a solution.

Now, with the solution of the PWD equation, we can write for an arbitrary regular function $g(x_1)$,

$$\left\langle g(x_1) \frac{\partial \bar{H}}{\partial x_1} \right\rangle = T \left\langle \frac{dg}{dx_1} \right\rangle \quad (48)$$

(law of equipartition of energy). Since, in our \bar{H} , x_2 is separated, we can set

$$\psi(x_1, x_2) = \rho(x_1)\phi(x_2), \quad (49)$$

where ϕ is the Gaussian distribution with $\langle x_2^2 \rangle = \sigma_0^2$ and $\langle x_2 \rangle = 0$. In Eq. (48), the average can thus be calculated only with respect to $\rho(x_1)$.

Since, in Eq. (48), g is arbitrary, we obtain an infinite series of equations of the form

$$\left\langle x_1^n \frac{\partial \bar{H}}{\partial x_1} \right\rangle = nT \langle x_1^{n-1} \rangle, \quad (50)$$

where n is a nonnegative integer:

$$\left\langle v_s x_1 + \frac{1}{2\pi} f(x_1) \right\rangle = 0 \quad (n=0), \quad (51)$$

$$\left\langle v_s x_1^2 + \frac{1}{2\pi} x_1 f(x_1) \right\rangle = T \quad (n=1), \quad (52)$$

$$\left\langle v_s x_1^3 + \frac{1}{2\pi} x_1^2 f(x_1) \right\rangle = 2T \langle x_1 \rangle \quad (n=2), \quad (53)$$

and so on. Notice that Eq. (51) agrees with Eq. (39) for Gaussian ρ . Likewise, when ρ is assumed Gaussian, Eq. (52) gives Eq. (40). It is interesting to see that two independent methods lead to the same result.

In order to go beyond the Gaussian approximation, let us introduce the cumulant expansion

$$\ln \bar{\rho}(k) = \sum_{n=1}^{\infty} \frac{(ik)^n}{n!} C_n, \quad (54)$$

where

$$\bar{\rho}(k) = \int_{-\infty}^{\infty} dx e^{ikx} \rho(x). \quad (55)$$

Here C_n is n th cumulant.⁸ When ρ is Gaussian, all C_n ($n > 2$) are zero and $C_1 = X_1$, $C_2 = \sigma_{11}$. When ρ is not very different from a Gaussian, we may terminate the expansion at some n . This is plausible, but without proof.

Let us terminate Eq. (54) at $n=3$ and also terminate the series of Eq. (50) at $n=2$. We can thus evaluate the averages in Eqs. (51) and (52) by a Fourier transformation technique. The results are

$$v_s C_1 + \frac{f_0}{4\pi} = 0, \quad (56)$$

$$v_s (C_2 + C_1^2) + \frac{f_0}{4\pi} \left(C_1 + \frac{\sqrt{C_2}}{\sqrt{\pi}} \right) = T, \quad (57)$$

$$v_s (C_3 + 3C_1 C_2 + C_1^3) + \frac{f_0}{4\pi} (C_2 + C_1^2) + \frac{f_0}{4\pi^2} \left(\frac{\sqrt{\pi} C_3}{2\sqrt{C_2}} + 2\sqrt{\pi} C_1 \sqrt{C_2} \right) = 2TC_1. \quad (58)$$

The first two of these are the same as in the case of the Gaussian approximation, and the solution of Eq. (58) is $C_3 = 0$! This explains why the Gaussian approximation fits the solution of the PWD equation so well. For another wake function (a resonator, for example), C_3 does not generally vanish.

5. DISCUSSION

We have shown that, when the wake force is localized, we should not use the FP equation with the time-dependent Hamiltonian H , Eq. (1), unless some regularization accompanies it. Instead, we can construct another theory based on a set of mappings. In fact, using a Gaussian approximation, Eq. (29), and a constant wake, Eq. (30), we can construct a soluble model.

Based on these results, some further discussion is in order.

5.1. Multiparticle Tracking

Let us begin by comparing the results of our model to those of MPT.² In MPT we start with an appropriate initial distribution, such as

$$\psi_{\text{initial}} = \frac{1}{N_p} \sum_{l=1}^{N_p} \delta(x_1 - x_{1l}) \delta(x_2 - x_{2l}), \quad (59)$$

$$x_{il} = \sigma_0 \hat{P}_l, \quad (60)$$

where \hat{P}_l is a Gaussian random noise, as before, and N_p is the number of super-particles. We operate the mapping, Eqs (9)–(11), on each of the x_{il} many times (more than several damping times).

With a large enough N_p , MPT gives almost unique results. In Fig. 4, we show a result of MPT, together with the results of our model and of the PWD equation for comparison, both using the parameters shown in Table I. The figure tells us, first, that although numerical agreement between MPT and our model is not good, qualitative features agree very well: In particular, (i) σ_{11}^∞ decreases first and begins to increase at some f_0 , (ii) σ_{22}^∞ increases as f_0^2 from the beginning, and (iii) σ_{12}^∞ behaves in almost the same manner. Second, we see that for σ_{11}^∞ there is a certain difference between MPT and the PWD, even for small f_0 .

As for the dipole motion, the fixed point X_i^∞ in Eq. (34) agrees very well with the results of MPT, or course. Now, let us notice from Eqs. (33) and (34) that the motion of X_i around X_i^∞ is independent of f_0 . A spectrum analysis performed in MPT shows that there is no noticeable variation of the Fourier spectrum of X_i ; that is, there is no synchrotron tune shift. This result is completely consistent with our model.

5.2. MPT vs the PWD Equation

As stated above, there is a certain numerical difference between the results for MPT and the PWD equation with regard to σ_{ij} (both are numerical results). It is

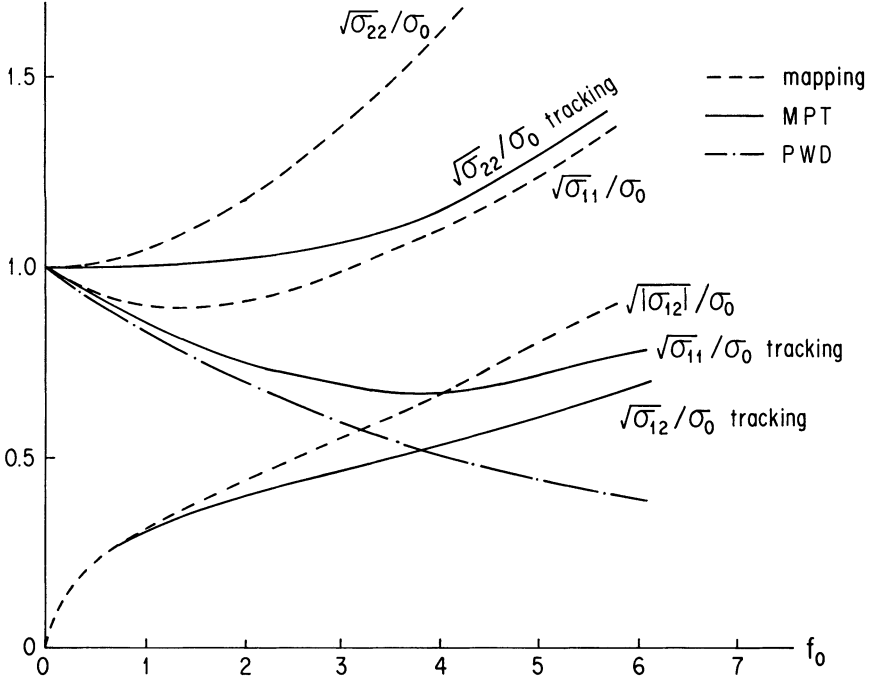


FIGURE 4 σ_{ij} of the equilibrium distribution obtained by multiparticle tracking (solid line) with the parameters listed in Table I. σ_{ij}^{∞} of the mapping equations and σ_{11} from the PWD equation are also shown for comparison. The abscissa is labeled in units of 10^{-3} .

natural to explain this difference by time-dependence: MPT represents H , Eq. (1), while the PWD equation represents \bar{H} , Eq. (5). In fact, when we introduce N_s into MPT, the resulting σ_{ij} is closer to that of the PWD equation.

This observation seems to be quite contrary to that given by Renieri,³ where almost the same comparison is done using a somewhat more realistic wake function, an exponentially damping wake. In Ref. 3, Renieri shows that numerical results for σ_{11} and σ_{22} from the PWD equation agree well with MPT. The difference between Renieri and the present paper seems to come from the difference of ν_s : He used $\nu_s = 0.01$, one order of magnitude smaller than ours.

In a sense, the time dependence means that the bunch ellipse rotates by $2\pi\nu_s$ between nonlinear kicks. *Wake*. When ν_s is small, this effect does not appear strongly. In fact, the limit $\nu_s \rightarrow 0$ provides another means of reaching the PWD equation result, Eq. (40), from the mapping results, Eq. (36). In Eq. (36), the contribution of b becomes negligible relative to a ; When we notice that $\xi \leq 1$, Eq. (36) reduces to Eq. (40). At the same time, the value of f_0 which gives the same σ_{11} becomes much smaller; this implies that σ_{12} and σ_{22} do not deviate much from the natural values. We may say that when ν_s is not small enough (this is the case for large electron rings), MPT can predict different behavior from the solution of the PWD equation.

The difference of the wake function should also be considered in comparing Renieri's results with ours. This effect, however, seems not to be qualitatively significant in the present case.

In conclusion, the PWD equation and MPT can give different results when (i) the wake force is large enough, (ii) N_s is not large, or (iii) v_s is not small.

5.3. Gaussian Approximation vs MPT

The fact that our model is soluble is partly due to the Gaussian approximation (GA). On the other hand, the GA is to some extent not physical: Even starting from the Gaussian ψ , it will produce non-Gaussian finer structure after nonlinear mappings such as *Wake*.

The results of MPT show that our model almost always estimates σ_{11} larger than MPT. Here we explain why. The entropy S , defined by Eq. (43), has the remarkable property that it should not change under any (linear or nonlinear) mapping if it is symplectic. Thus, under *Wake*, Eq. (11), S should not change: The active ψ [which determines $f(x_1)$] should not be considered as changing, as discussed below Eq. (18). Thus *Wake* is symplectic, though H is not the usual Hamiltonian. On the other hand, $S = \text{const} + (\ln \det \sigma)/2$ in the GA: S always increases in *Wake* in our GA. Of course, the increase of $\det \sigma$ is not forbidden and is expected for nonlinear mappings. We are led to the conclusion that our model suffers from an unavoidable unphysical heating due to the loss of information entailed by the GA; that is, ψ is unavoidably “expanded” in order to fit a non-Gaussian structure within the framework of the GA. Our model thus generally gives σ_{ij} some unphysical part. The unphysical part is small for small T_e and small f_0 . Such an unphysical bunch lengthening seems inevitable when we work with some approximation of ψ .

5.4. The GA vs the PWD Equation

As stated in Section 3, our GA model predicts qualitatively different behavior for σ_{ij} than does the PWD equation. Since we could rederive the PWD equation results by letting $N_s \rightarrow \infty$, it seems almost certain that our model, based on the mapping formulation, is a time-dependent extension of the PWD equation. At the same time, from the discussion in Section 4, it seems that the GA is not always a good approximation. In some cases, higher-order cumulants, for example, will be needed.

5.5. The Conventional Theory vs MPT

In the conventional mode-coupling theory (MCT),⁴ it is thought that (i) the dynamics is governed by the time-independent FP equation, Eq. (6), whereas almost all other papers work with the Vlasov equation because of its simplicity (Suzuki⁹ has shown that there is no large difference in either the instability or I_{th}); (ii) when the wake force is weak (low current), ψ is given by the solution of the PWD equation (basic distribution), which is stable; (iii) when the wake force

becomes large ($I > I_{\text{th}}$), a small disturbance of ψ around the basic distribution increases, leading to a bunch lengthening; (iv) the lengthened bunch is again stable¹⁰ as long as the wake force is less than the next critical value; and so on. The critical value (or I_{th}) is determined by mode coupling.

As stated above, our results for MPT seem to show qualitatively different behavior from MCT. In fact, MCT predicts¹¹ that our system becomes unstable when $f_0 \geq 2.61 \times 10^{-3}$, owing to a mode coupling between modes¹ $m = 1$ and $m = -1$. This is far from the predictions given by our MPT (no threshold and no tune shift). In particular, the increase of the energy spread seems not to imply a mode coupling.

One point should be noted here. In the application of MCT, we used an approximation that the solution of the PWD equation is Gaussian with $\sigma_{ij} = \sigma \delta_{ij}$ (σ is an input parameter), quite contrary to the results of MPT and our model, in order to numerically calculate coefficients of the linearized Vlasov equation. This seems to be at least one of the reasons why the numerical results of the MCT disagree with MPT.

There now exist MPT results which show behavior qualitatively consistent with MCT; for example, Refs. 12 and 13 deal with simulations for SPEAR. At the same time, there are also MPT publications showing behavior inconsistent with MCT. For example, Ref. 14 deals with PETRA: The energy spread grows almost as I^2 from $I = 0$. These results seem to fit the experimental data well. One possible source of difference between these MPT results is the difference in v_s : $v_s(\text{SPEAR}) \cong 0.03$ while $v_s(\text{PETRA}) \cong 0.08$. The discussion of Section 5.2 holds true here also.

It seems that little has been done on detailed comparison of MPT and MCT results. Since there are some approximations involved in both MPT (finite number of super-particles, method to calculate wake forces, and so on) and MCT (finite number of modes included, simplification of the basic distributions, and so on), the comparison seems necessary, at least for some simple wake functions.

As for the constant wake, as shown above, there is a qualitative difference. Even when the superperiod $N_s = 20$ is used in MPT, no threshold behavior appears. This implies that the disagreement between MPT and MCT does not come from the time-dependence alone. Since there seems to be no reason that the constant wake should be an exceptional case, we should expect the same for more general wake functions. We are, however, obliged to relegate the study of this problem to the future investigation, since it is another difficult problem.

In conclusion, when (i) the wake source is localized, (ii) the wake force is large, and (iii) v_s is not small, we must at least modify the conventional MCT to incorporate the effects of localization by employing Eq. (28), for example, more seriously including effects on the PWD equation.

5.6. Threshold Behavior

In our model so far we have seen no threshold behavior for σ_{ij}^∞ . (And this is consistent with MPT.) Of course, this should not be extended to a general wake

force. The absence of a threshold is not a consequence of the mapping formulation.

In tracking σ_{ij} in our GA model according to Eq. (35), there is no *a priori* reason that the mapping has a stable period-1 fixed point. For the nonlinear deterministic mapping, we often encounter chaotic behavior.¹⁵ In the case of a general wake force, it is thus possible that there is a series of threshold current $I_{\text{th}}^{(1)}, I_{\text{th}}^{(2)}, \dots$, at which a stable period- n fixed point becomes unstable and a new pair of stable period- $2n$ fixed points appear (bifurcation). It is also possible, in some cases, that the behavior of $X_i, \sigma_{ij}, \sigma_{jk}, \dots$ becomes chaotic at some critical current. In such cases, we have an interesting turbulentlike model. This is only a conjecture, of course.

Let us, hereafter, confine ourselves to the case where the period-1 fixed point is stable. In MCT, I_{th} is related to the coupling of coherent modes of ψ . It is clear that our GA model cannot incorporate such higher-order coherent modes, owing to the lack of degrees of freedom. This fact limits the applicability of our model. In order to expand our model, we must (i) set

$$\psi = \psi_0 + \sum_n a_n f_n(x_1, x_2),$$

where ψ_0 is the period-1 fixed distribution of the mappings, such as Eqs. (9)–(11), and f_n belongs to a complete orthonormal system; (ii) obtain a mapping equation for a_n ; (iii) linearize the mapping equation around ψ_0 ; and (iv) use the eigenvalue technique.

As is easily seen, this is a natural extension of the conventional theory to the time-dependent case. This must also be relegated to a future investigation.

5.7. Constant Wake Function

We use the constant wake function in order to present our method. This enabled us to construct an analytically soluble model. This wake function is, however, too simple to simulate realistic situations. If we can construct a soluble model (with the GA or not) with more realistic wake functions, it will be quite interesting and valuable.

5.8. Actual Storage Rings

It is now clear that when the wake source is localized the mapping formulation works well, while the conventional method is not applicable. On the other hand, when the sources are to be treated as smoothed throughout the ring, the conventional method is enough.

For an actual storage ring, each source of short-range wake forces (broadband impedance) is localized, but sources are distributed throughout the ring. It seems that the mapping formulation represents a limit of gathering the sources into N_s points, while the conventional method represents a limit of averaging the sources

throughout the ring. (N_s does not necessarily correspond to the actual superperiodicity.) Since results for the two limits disagree with one another, we must be very careful in treating the wake force. In particular, MPT, with wake sources gathered into a few points in the ring (this is a usual method to reduce the CPU time to a reasonable total) may, in some cases, be unrealistic.

An analogy seems useful here: For single-particle tracking with nonlinear elements, we must not group the elements into some smaller number of points. In this case, however, there is a somewhat reasonable approximation method¹⁶ that does group nonlinear elements. In our case, there is no such method yet. In order to check whether a time-averaging approximation is permissible or not, rigorously speaking, we must compare the results with time-dependent and fully realistic MPT. There seems to be no *a priori* justification for time-averaging.

6. CONCLUSION

When the wake force sources are to be treated as fully localized, the conventional theory based on the usual Fokker-Planck equation is not applicable directly. Instead, we propose a mapping method, which shows good qualitative agreement with multiparticle tracking for a simple example. The conventional method and the present one represent different limits of the actual dynamics. Since our model can rederive the results of the conventional method by letting the superperiodicity become infinite, our method seems more general. It is hoped that the mapping method, though too limited at the present stage, will provide a new and powerful tool for the analytical (algebraic) study of collective beam dynamics.¹⁷

ACKNOWLEDGMENTS

The author would like to thank Dr. K. Yokoya for many helpful discussions and for kindly recommending the use of his computer program. The author is also indebted to Professor T. Suzuki for a careful reading of the manuscript. Finally, the author wishes to thank Dr. F. Ruggiero for showing him an interesting regularization idea.

REFERENCES

1. A. W. Chao, *AIP Conf. Proc.* **157**, 353 (1983) and references quoted therein.
2. K. Hirata, KEK internal report 85-3 (1985) (in Japanese).
3. A. Reinieri, Laboratori Nazionali di Frascati del CERN, report NO. LNF-75/11R (1976) and H. G. Hereward, PEP Note No. 53 (1973), quoted therein.
4. F. Sacherer, *IEEE Trans. Nucl. Sci.* **NS-24**, 1393 (1977) and Ref. 1.
5. F. Ruggiero, LEP Note 567 (1986).
6. F. Ruggiero, *Particle Accelerators* **20**, 45 (1986).
7. A. W. Chao and R. D. Ruth, *Particle Accelerators* **16**, 201 (1984).
8. See, for example, Shang-Keng Ma, *Statistical Mechanics* (World Scientific, Philadelphia, 1985).
9. T. Suzuki, *Particle Accelerators* **14**, 91 (1983).

10. B. Zotter, *IEEE Trans. Nucl. Sci.* **NS-28**, 2602 (1981).
11. We used the computer code of K. Yokoya, which is based on T. Suzuki, Y. Chin, and K. Satoh, *Particle Accelerators* **13**, 179 (1983).
12. P. B. Wilson, K. Bane, and K. Satoh, *IEEE Trans. Nucl. Sci.* **NS-28**, 2525 (1981).
13. R. Siemann, *Nucl. Instrum. Methods* **203**, 57 (1982).
14. T. Weiland, DESY report 81-088 (1981).
15. See, for example, A. J. Lichtenberg and M. A. Lieberman, *Regular and Stochastic Motion* (Springer, New York, 1983).
16. A. J. Dragt, *AIP Conf. Proc.* **87**, 147 (1982).
17. K. Hirata, *Phys. Rev. Lett.* **58**, 25 (1987).

APPENDIX A

An Idea for Regularizing the Differential Equations for Moments

Here we give one simple regularization of Eq. (23), due to Ruggiero,⁵ which can be used to rederive Eq. (20), but cannot be extended to higher-order moments. In Eq. (23), Ruggiero defines the right-hand side as

$$\frac{d}{d\theta} \langle x_2^2 \rangle = -2 \frac{\langle x_2 f \rangle_+ + \langle x_2 f \rangle_-}{2} \delta(\theta). \quad (\text{A-1})$$

Notice that, by analogy to the case of Eq. (22),

$$\frac{d}{d\theta} \langle x_2 f \rangle = -\langle f^2 \rangle \delta(\theta), \quad (\text{A-2})$$

the right-hand side of which is unambiguous. From this we have

$$\langle x_2 f \rangle_+ = \langle x_2 f \rangle_- - \langle f^2 \rangle. \quad (\text{A-3})$$

Using this in Eq. (A-1), we have

$$\langle x_2^2 \rangle_+ = \langle x_2^2 \rangle_- - 2\langle x_2 f \rangle_- + \langle f^2 \rangle, \quad (\text{A-4})$$

the right-hand side of which is the same expression as in Eq. (20).

Now, let us apply it to $\langle x_2^3 \rangle$:

$$\frac{d}{d\theta} \langle x_2^3 \rangle = -3\langle x_2^2 f \rangle \delta(\theta) \quad (\text{A-5})$$

is easily derived using Eq. (21). This now should be

$$\frac{d}{d\theta} \langle x_2^3 \rangle = -3 \frac{\langle x_2^2 f \rangle_+ + \langle x_2^2 f \rangle_-}{2} \delta(\theta). \quad (\text{A-6})$$

We also have

$$\begin{aligned} \frac{d}{d\theta} \langle x_2^2 f \rangle &= -2\langle x_2 f^2 \rangle \delta(\theta) \\ &= -(\langle x_2 f^2 \rangle_+ + \langle x_2 f^2 \rangle_-) \delta(\theta), \end{aligned} \quad (\text{A-7})$$

$$\frac{d}{d\theta} \langle x_2 f^2 \rangle = -\langle f^3 \rangle \delta(\theta). \quad (\text{A-8})$$

From Eq. (A-8), we obtain

$$\langle x_2 f^2 \rangle_+ = \langle x_2 f^2 \rangle_- - \langle f^3 \rangle,$$

which is inserted to Eq. (A-7) to give

$$\langle x_2^2 f \rangle_+ = \langle x_2^2 f \rangle_- - (2\langle x_2 f^2 \rangle - \langle f^3 \rangle). \quad (\text{A-9})$$

Inserting this into Eq. (A-6), we obtain

$$\begin{aligned} \langle x_2^3 \rangle_+ &= \langle x_2^3 \rangle_- - \frac{3}{2} (\langle x_2^2 f \rangle_+ + \langle x_2^2 f \rangle_-) \\ &= \langle x_2^3 \rangle_- - \frac{3}{2} (2\langle x_2^2 f \rangle_- - 2\langle x_2 f^2 \rangle_- + \langle f^3 \rangle) \\ &= \langle x_2^3 \rangle_- - 3\langle x_2^2 f \rangle + 3\langle x_2 f^2 \rangle - \frac{3}{2} \langle f^3 \rangle, \end{aligned} \quad (\text{A-10})$$

which, however, does not agree with the correct expression

$$\langle x_2^3 \rangle_+ = \langle (x_2 - f)^3 \rangle_-.$$

It seems almost clear now that the regularization of Ruggiero, though interesting and ingenious, cannot be applied to higher-order moments. As we said in the text, our generalized FP equation can rederive all the right expressions for higher-order moments.

If we can find a simple and reliable regularization scheme for moments, it will be quite valuable. Ruggiero's argument seems to be interesting as the starting point and, at the same time, illustrates the difficulty.

APPENDIX B

An Alternative Regularization of the Fokker-Planck Equation with Localized Wake Force

Since the arguments leading to Eq. (27) are somewhat technical, a more physically intuitive discussion seems desirable. In physical systems, $\delta(\theta)$ is an ideal limit, let alone in the case of MPT.

Now, let us examine the case

$$H_1 \delta(\theta) = \lim_{\varepsilon \rightarrow 0} H_1 \frac{1}{\varepsilon} \quad (\text{for } \leq \theta \leq \varepsilon). \quad (\text{B-1})$$

That is, we expand the "distance" between 0^- and 0^+ to ε , and let ε be zero afterwards. We now have

$$\dot{\psi} = \frac{1}{\varepsilon} [H_1, \psi] = \frac{1}{\varepsilon} \frac{\partial \psi}{\partial x_2} f(x_1). \quad (\text{B-2})$$

Then, instead of Eq. (23), we obtain

$$\frac{d}{d\theta} \langle x_2^2 \rangle = -2 \langle x_2 f \rangle \frac{1}{\varepsilon}. \quad (\text{B-3})$$

At the same time,

$$\frac{d}{d\theta} \langle x_2 f \rangle = -\langle f^2 \rangle \frac{1}{\varepsilon} \quad (\text{B-4})$$

holds. Since $\langle f^2 \rangle$ is θ -independent, we can integrate Eq. (B-4) to obtain

$$\langle x_2 f \rangle_\theta = \langle x_2 f \rangle_0 - \langle f^2 \rangle \frac{\theta}{\varepsilon}. \quad (\text{B-5})$$

Thus, Eq. (B-3) is

$$\frac{d}{d\theta} \langle x_2^2 \rangle = -\frac{2}{\varepsilon} \left(\langle x_2 f \rangle_0 - \langle f^2 \rangle \frac{\theta}{\varepsilon} \right), \quad (\text{B-6})$$

which can be further integrated to give

$$\langle x_2^2 \rangle_\theta = \langle x_2^2 \rangle_0 - 2 \langle x_2 f \rangle_0 \frac{\theta}{\varepsilon} + \langle f^2 \rangle \left(\frac{\theta}{\varepsilon} \right)^2. \quad (\text{B-7})$$

By letting $\theta = \varepsilon$ and identifying

$$\begin{aligned} \lim_{\varepsilon \rightarrow 0} \langle \quad \rangle_\varepsilon &= \langle \quad \rangle_+, \\ \langle \quad \rangle_0 &= \langle \quad \rangle_-, \end{aligned} \quad (\text{B-8})$$

we then reproduce Eq. (20). The same argument can be repeated for any higher moments. Notice here that the limit $\varepsilon \rightarrow 0$ should be taken at the final stage of calculation.

We can further show the equivalence of Eqs. (27) and (B-2). The latter implies that

$$\psi(x_1, x_2, \theta) = \psi \left[x_1, x_2 + f(x_1) \frac{\theta}{\varepsilon}, 0 \right] \quad (\text{B-9})$$

for $0 \leq \theta \leq \varepsilon$. By letting $\theta \rightarrow \varepsilon$ and $\varepsilon \rightarrow 0$, we obtain Eq. (26), which implies Eq. (27). In this respect, the formal equation, Eq. (21), corresponds to letting $\varepsilon \rightarrow 0$ in the first stage.

Although this regularization is physically and mathematically sound, it spoils the original simplification sought in the ‘‘thin lens approximation.’’

APPENDIX C

A Derivation of σ_{ij}^∞

Here we show how to obtain the period-one fixed point, Eq. (36), of the mapping system, Eq. (35). We use the notation,

$$\sigma_{ij} \xrightarrow{\text{Radiation}} \sigma'_{ij} \xrightarrow{\text{Wake}} \sigma''_{ij} \xrightarrow{\text{Oscillation}} \sigma'''_{ij}. \quad (\text{C-1})$$

The period-one fixed point σ_{ij}^∞ is the solution of $\sigma_{ij} = \sigma'''_{ij}$.

Notice that $\det \sigma$ and $\text{Tr} \sigma$ are invariant under *Oscillation*, and σ_{11} is invariant

under *Radiation* and *Wake*. We then easily obtain

$$\det \sigma''' = \xi^2 \det \sigma + (1 - \xi^2) \sigma_0^2 \sigma_{11} + \frac{\pi - 3}{12\pi} f_0^2 \sigma_{11}, \quad (\text{C-2})$$

$$\text{Tr } \sigma''' = \text{Tr } \sigma + (\xi^2 - 1)(\sigma_{22} - \sigma_0^2) - \frac{\xi f_0 \sigma_{12}}{(\pi \sigma_{11})^{1/2}} + \frac{f_0^2}{12}, \quad (\text{C-3})$$

$$\begin{aligned} \sigma'''_{11} &= \sigma_{11} \cos^2 \Delta \phi \\ &+ \left\{ [\xi^2 \sigma_{22} + (1 - \xi^2) \sigma_0^2] - \frac{\xi f_0 \sigma_{12}}{(\pi \sigma_{11})^{1/2}} + \frac{f_0^2}{12} \right\} \sin^2 \Delta \phi \\ &+ 2 \left(\xi \sigma_{12} - \frac{f_0}{2\sqrt{\pi}} \sqrt{\sigma_{11}} \right) \sin \Delta \phi \cos \Delta \phi. \end{aligned} \quad (\text{C-4})$$

Eqs. (C-2) and (C-3) can be rewritten as

$$(1 - \xi^2)(X - Y^2) = \frac{\pi - 3}{12\pi} f_0^2, \quad (\text{C-5})$$

$$(1 - \xi^2)X = \frac{f_0^2}{12} - \frac{\xi f_0}{\sqrt{\pi}} Y, \quad (\text{C-6})$$

where $X = \sigma_{22} - \sigma_0^2$, $Y = \sigma_{12}/\sqrt{\sigma_{11}}$.

From these we have

$$Y = \frac{1}{2(1 - \xi^2)} \frac{f_0}{\sqrt{\pi}} (\pm 1 - \xi). \quad (\text{C-7})$$

Now, σ_{12} decreases under *Radiation* and *Wake*, so that σ_{12}^∞ should be positive after *Oscillation*. We thus take the plus sign in Eq. (C-7). Then we easily obtain

$$X = \frac{f_0^2}{12(1 - \xi^2)^2 \pi} [(1 - \xi^2)\pi - 6\xi(1 - \xi)], \quad (\text{C-8})$$

which leads to σ_{22}^∞ in Eq. (36).

Now, Eq. (C-4) is rewritten as

$$\begin{aligned} \sigma'''_{11} &= \xi^2 X + \sigma_0^2 - \frac{f_0 \xi}{\sqrt{\pi}} Y + \frac{f_0^2}{12} \\ &+ 2 \left(\xi Y - \frac{f_0}{2\sqrt{\pi}} \right) \cot \Delta \phi (\sigma_{11})^{1/2}. \end{aligned} \quad (\text{C-9})$$

This has a solution

$$(\sigma_{11})^{1/2} = -af_0 \pm [\sigma_0^2 + (a^2 + b)f_0^2]^{1/2}, \quad (\text{C-10})$$

where a and b are given in Eq. (36). Since $(\sigma_{11})^{1/2}$ should be positive, at least for $f_0 = 0$, the plus sign should be employed.